Stochastic Gravitational-Wave Background

Guo Chin Liu
Department of Physics, Tamkang University

Open Data Workshop, April 18-20, 2024

Stochastic Background

Superposition of many faint, unsolved gravitational-wave signals

- Cosmological sources: phase transition, inflation, cosmic string…
- Astrophysics sources: CBC, Core collapse supernovae, rapidly rotating NS…

GW signals

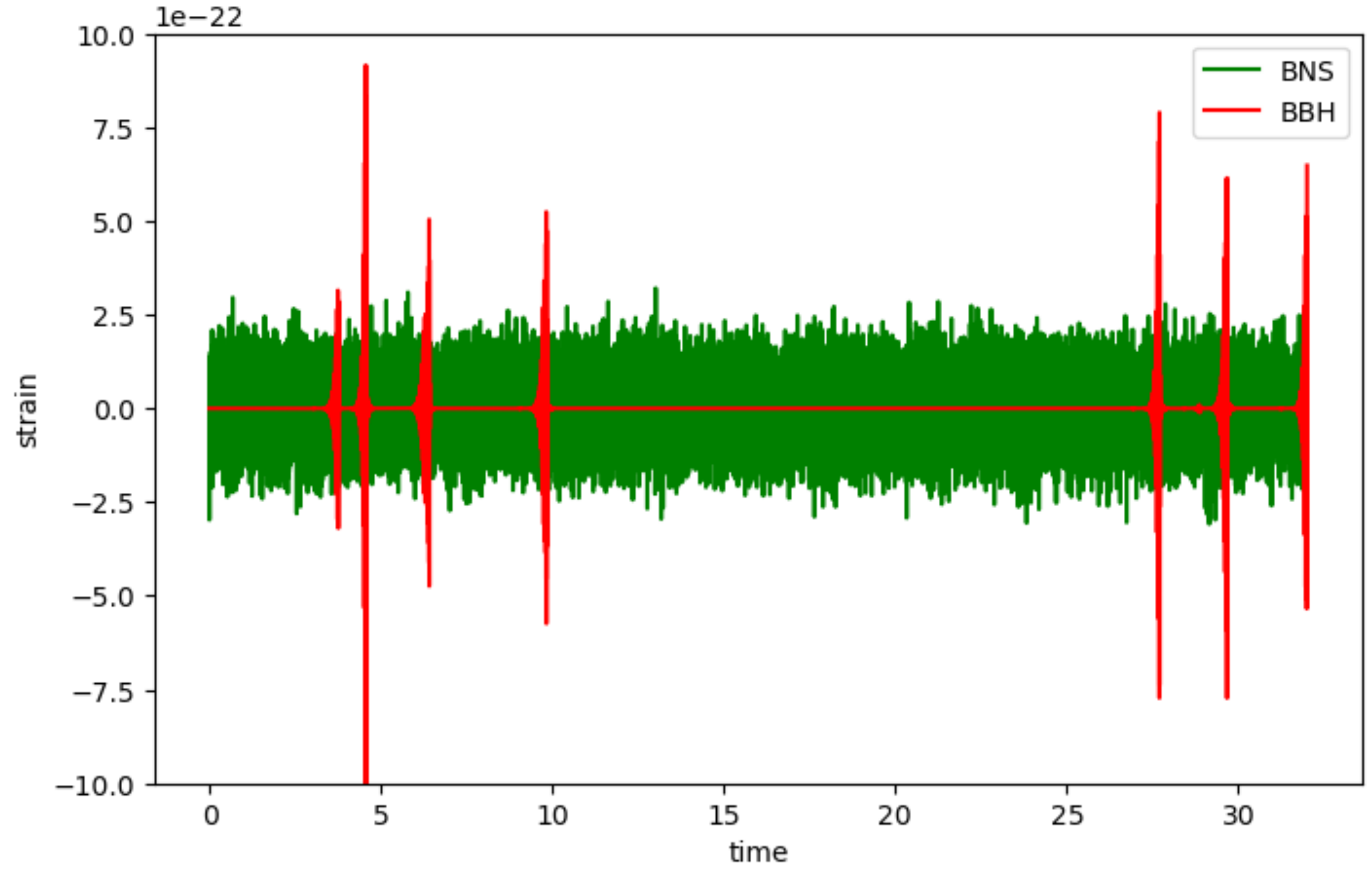

noise+GW signals

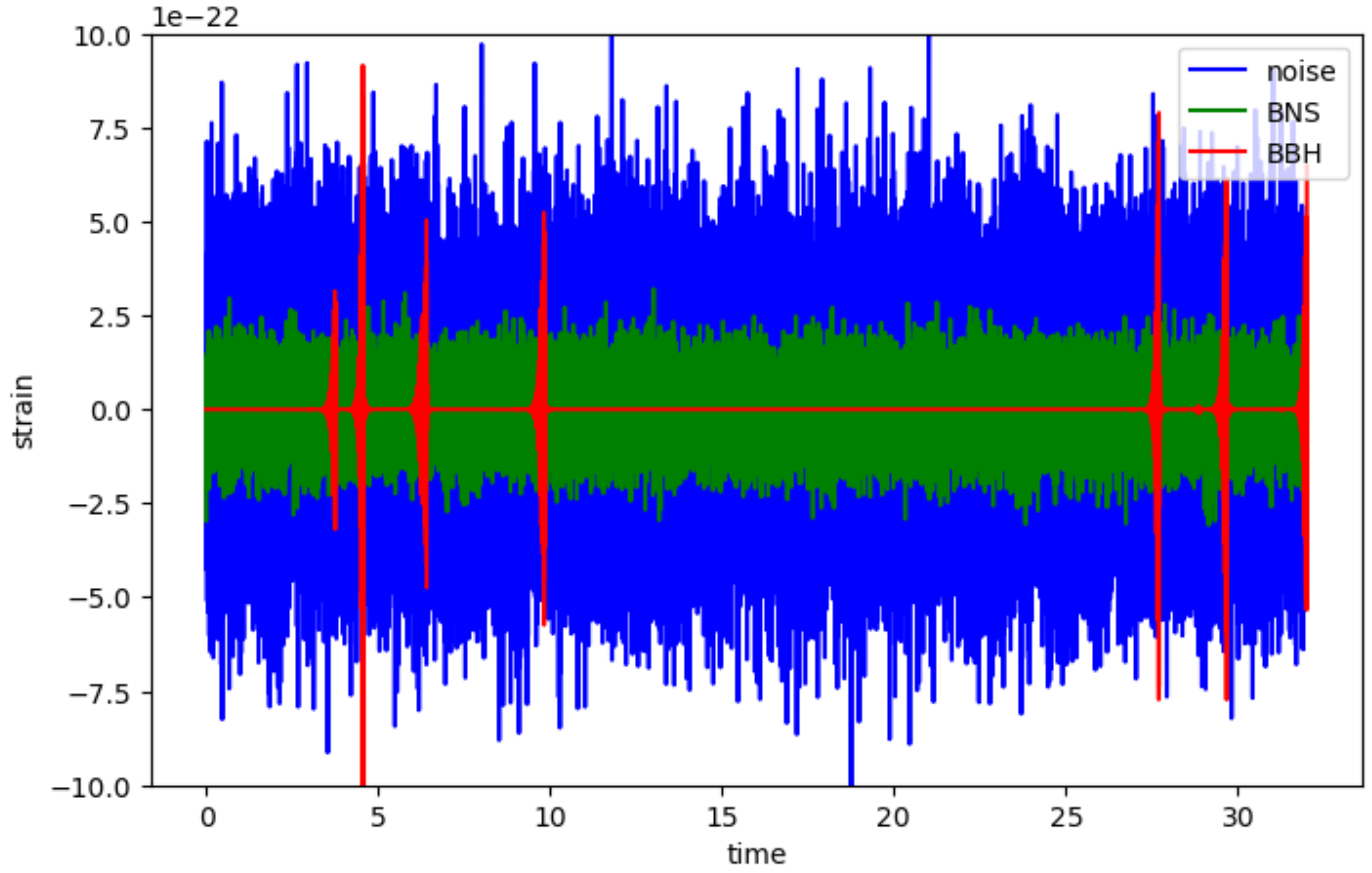

We study the statistical properties of the background

Plane wave expansion of metric perturbations

$$h_{ab}(t, \vec{x}) = \int_{-\infty}^{\infty} df \int d^2\Omega_{\hat{n}} \sum_{A=+,\times} h_A(f, \hat{n}) e_{ab}^A(\hat{n}) e^{i2\pi f(t+\hat{n}\cdot\vec{x}/c)}$$

- $\int_{-\infty}^{\infty} df$: **Integrate over frequencies**
- $\int d^2\Omega_{\hat{n}}$: **GW from all sky directions**
- $\sum_{A=+,\times}$: **Polarizations**
- $h_A(f, \hat{n})$: **Plane Wave coefficients**
- $e_{ab}^A(\hat{n})$: **Polarization tensors**

We can study the statistical properties of SGWB by measuring

$\left\langle h_{ab}(t, \vec{x}) \right\rangle$	⟺	$\left\langle h_A(f, \hat{n}) \right\rangle$
$\left\langle h_{ab}(t, \vec{x}) h_{cd}(t', \vec{x}') \right\rangle$	⟺	$\left\langle h_A(f, \hat{n}) h_{A'}(f', \hat{n}') \right\rangle$
$\left\langle h_{ab}(t, \vec{x}) h_{cd}(t', \vec{x}') h_{ef}(t'', \vec{x}'') \right\rangle$	⟺	$\left\langle h_A(f, \hat{n}) h_{A'}(f', \hat{n}') h_{A''}(f'', \hat{n}'') \right\rangle$

In the previous studies of SGWB, we assumed:

- The GW signals (and noise) are stationary Gaussian
- The GW signals are unpolarized
- Noise in different detectors is un-correlated

The rate of signals is large enough, the signal will be stationary Gaussian

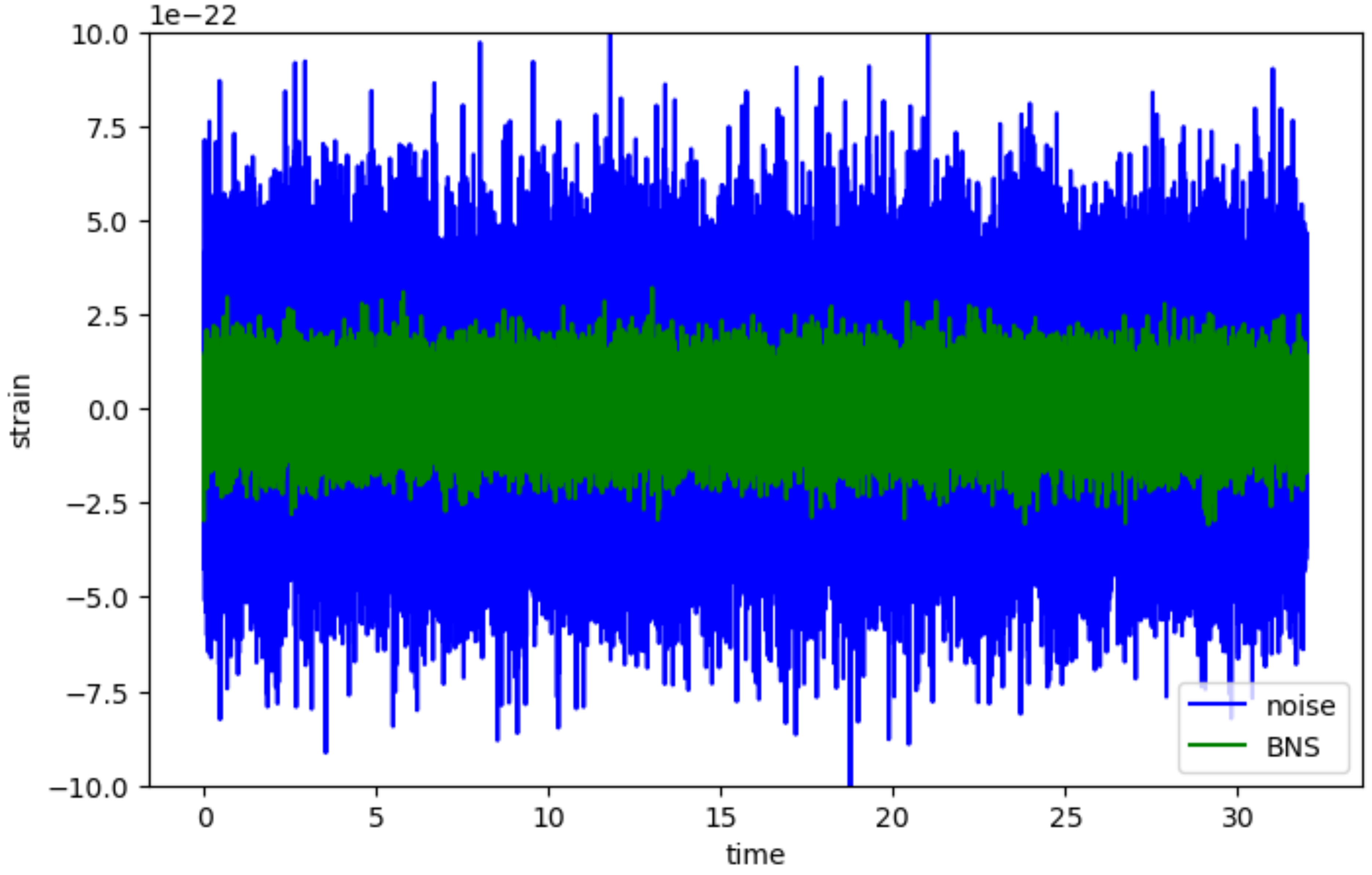

The rate of signals is small, the signals will be non-stationary and non-Gaussian

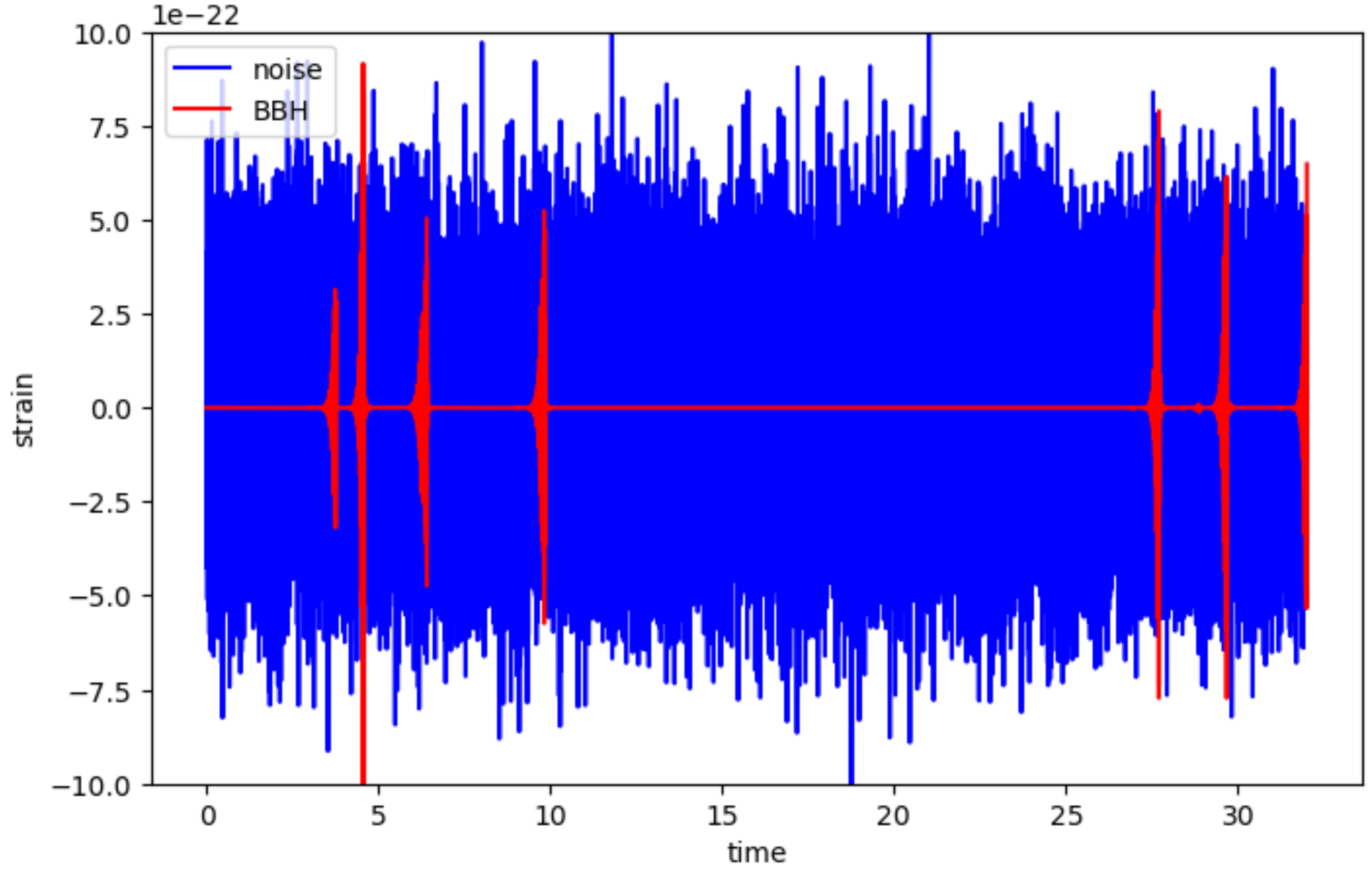

The Gaussian backgrounds are fully characterized by the quadratic expectation value. For non-Gaussian backgrounds, higher order moments are needed.

Gaussian Background

Quadratic expectation values

For a stationary, Gaussian, unpolarized and isotropic background:

$$\left\langle h_A(f,\hat{n})h^*_{A'}(f',\hat{n}')\right\rangle = \frac{1}{16\pi}S_h(f)\delta(f-f')\delta_{AA'}\delta^2(\hat{n},\hat{n}')$$

$S_h(f)$: one-sided GW strain power spectral density function

$$S_h(f) = \frac{3H_0^2}{2\pi^2}\frac{\Omega_{GW}(f)}{f^3}$$

$$\Omega_{GW}(f) \equiv \frac{1}{\rho_c}\frac{d\rho_{GW}}{d\ln f}$$

Fractional energy density spectrum in GW

For a stationary, Gaussian, unpolarized and anisotropic background:

$$\left\langle h_A(f,\hat{n})h^*_{A'}(f',\hat{n}')\right\rangle = \frac{1}{4}\mathscr{P}(f,\hat{n})\delta(f-f')\delta_{AA'}$$

$\mathscr{P}(f,\hat{n})$: spatial distribution pf GW power on the sky

What we try to learn from SGWB?

- Energy level of the isotropic GW background
  - Tensor and non-tensorial polarization background
  - Implications on cosmological and astrophysical models
- Anisotropic GW background
  - Any (detectable) GW signals from particular direction and/or at particular frequency (for example: due to the kinetic dipole or distribution of matter in local universe)
- Intermittent background
  - Learn the duty cycle and energy density contributed by BBH mergers.

$\Omega_{GW}(f)$

$$\Omega_{GW}(f) = \frac{1}{\rho_c} \int_0^\infty dz \frac{N(z)}{1+z} \left[f_r \frac{dE_{GW}}{df_r} \right]_{f_r = f(1+z)}$$

$N(z)$: number of GW emitters as function of z

f_r: emission frequency in the rest frame of the source

$\frac{dE_{GW}}{df_r}$: spectral energy density of a specific source

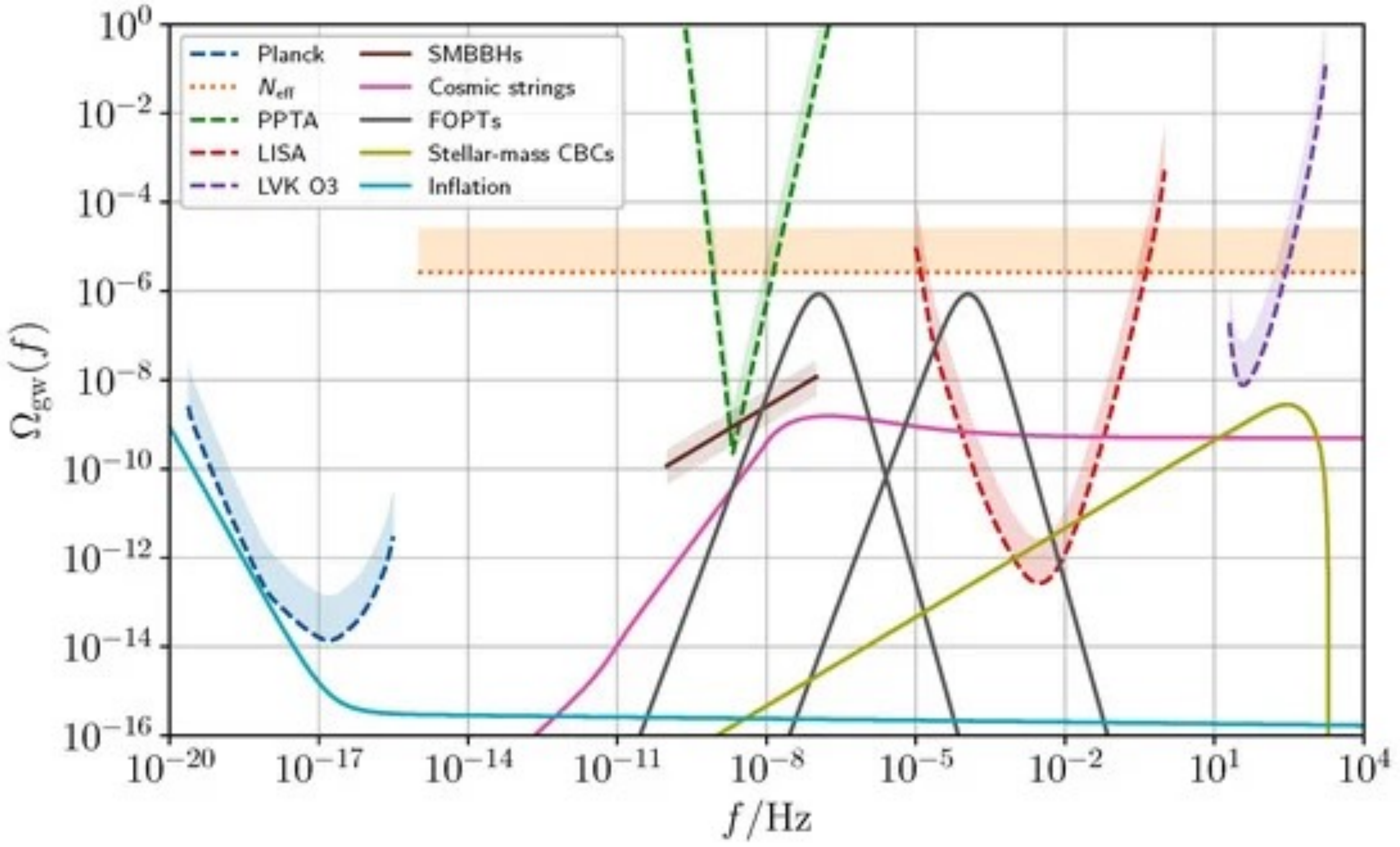

Rennin et al. 2022

The spectral dependence of a specific source is often reduced to a power law

$$\Omega_{GW}(f) = \Omega_{GW}(f_{\rm ref}) \left(\frac{f}{f_{\rm ref}} \right)^\alpha$$

Search Gaussian SGWB

SGWB contributes extra power on our data.

Problem: Distinguishing GW signals from noise in individual detectors is challenging.

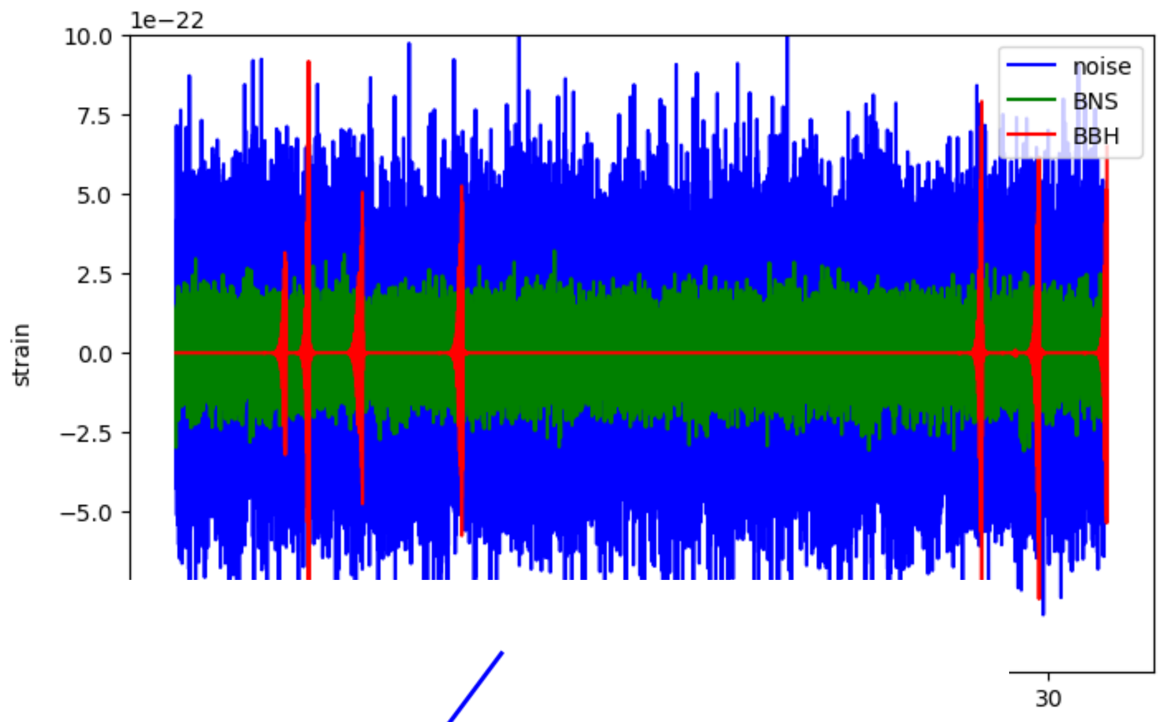

Solution: Cross-Correlation of the data from two detectors can suppress the uncorrelated noise

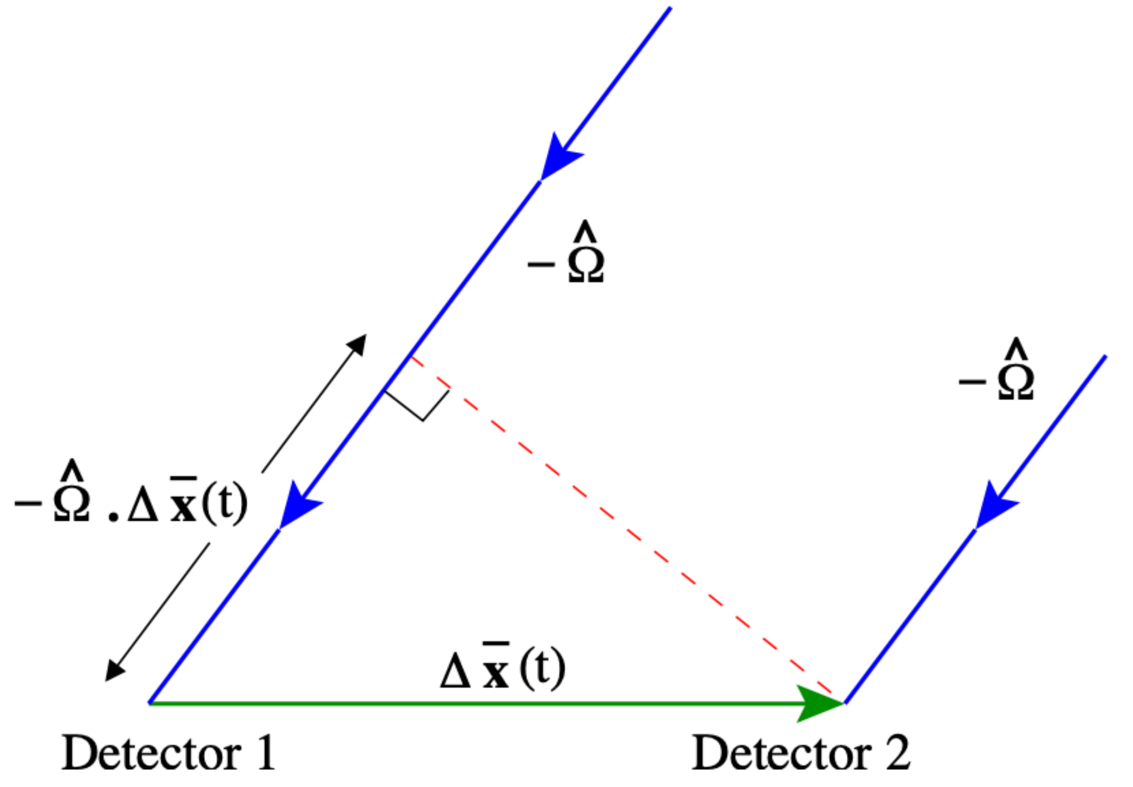

Ain, Suresh and Mitra 2018

Output in detector I : $\tilde{h}_I(f) = \int d^2\Omega_{\hat{n}} \sum_A R_I^A(f,\hat{n}) h_A(f,\hat{n})$

Detector response $R_I^A(f,\hat{n}) = \frac{1}{2}(u^a u^b - v^a v^b) e_{ab}^A(\hat{n})$

Cross-Correlation of two detectors I : $\langle C(f,t) \rangle = \frac{2}{\tau} \left\langle \tilde{h}_I(f,t) \tilde{h}_J^*(f,t) \right\rangle = H(f) \int_{S^2} d^2\theta \gamma(\hat{\theta},f,t) \mathscr{P}(\hat{\theta},f)$

$$\gamma(\hat{\theta},f,t) = \frac{1}{2} \sum_A F_1^A(\hat{\theta},t) F_2^A(\hat{\theta},t) e^{i2\pi f \hat{\theta}\cdot\Delta\vec{x}/c}$$

$\gamma(\hat{\theta},f,t)$: a geometry factor depends the separation of detectors and relative orientation of arms

Geometric factor H1-L1

- $\gamma(\hat{\theta}, f = 0, t)$, around the vicinity of two detectors, gives the size of field of view
- For higher frequencies, lines indicate regions with the same time delay to two detectors.
- Separation between the positive and negative lobes response provides the resolution of the image.
- The location of the positive and negative lobes are shifted relative to one another for the real and imaginary parts
- $\Delta\theta \simeq \dfrac{wavelength}{2\Delta x}$

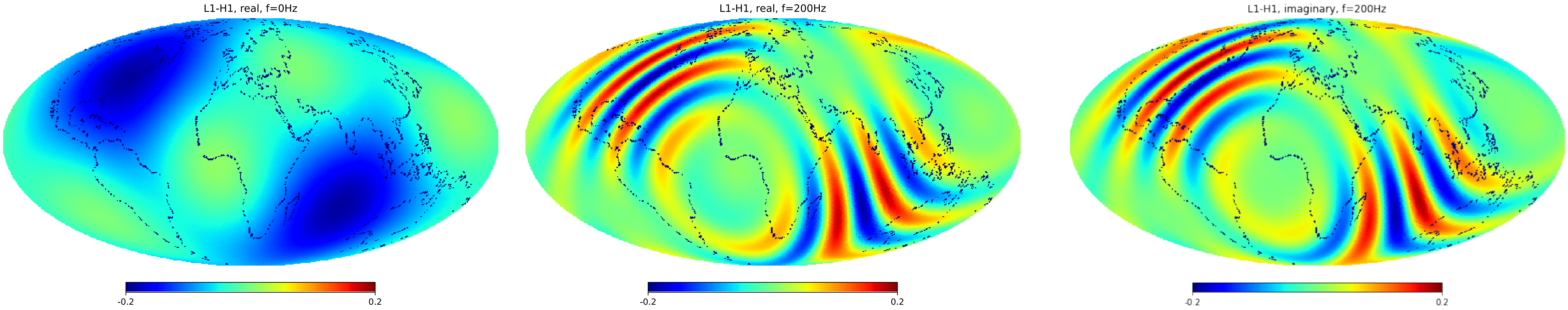

Geometric factor Virgo-KAGRA

- $\gamma(\hat{\theta}, f = 0, t)$, around the vicinity of two detectors, gives the size of field of view
- For higher frequencies, lines indicate regions with the same time delay to two detectors.
- Separation between the positive and negative lobes response provides the resolution of the image.
- The location of the positive and negative lobes are shifted relative to one another for the real and imaginary parts
- $\Delta\theta \simeq \dfrac{wavelength}{2\Delta x}$

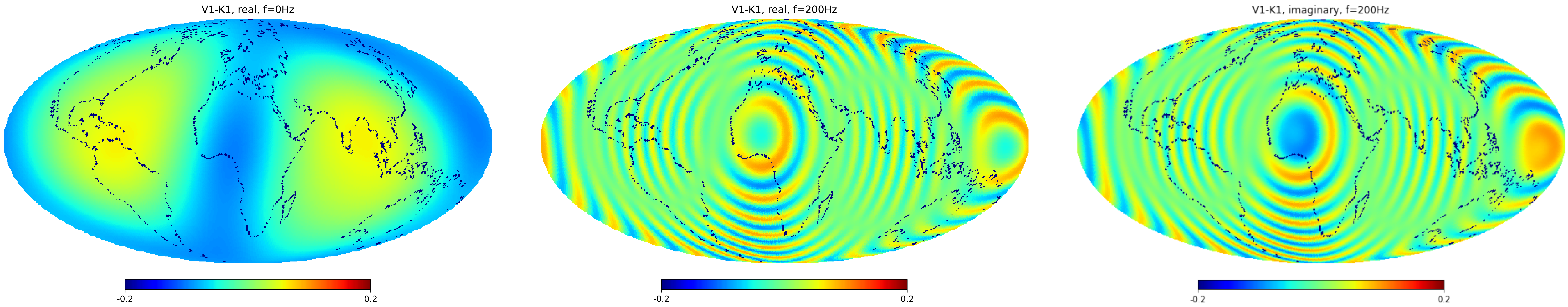

Isotropic Background

$$\Gamma_{IJ}(f) = \frac{1}{8\pi}\int d^2\Omega_{\hat{n}} \sum_A F_I^A(\hat{\theta}, t) F_J^A(\hat{\theta}, t) e^{i2\pi f \hat{\theta}\cdot\Delta\vec{x}/c}$$

$\Gamma_{IJ}(f)$ is the so-called overlap function of two detectors. It is like the transfer function between GW strain power $S_h(f)$ and cross power $\langle C(f,t)\rangle$

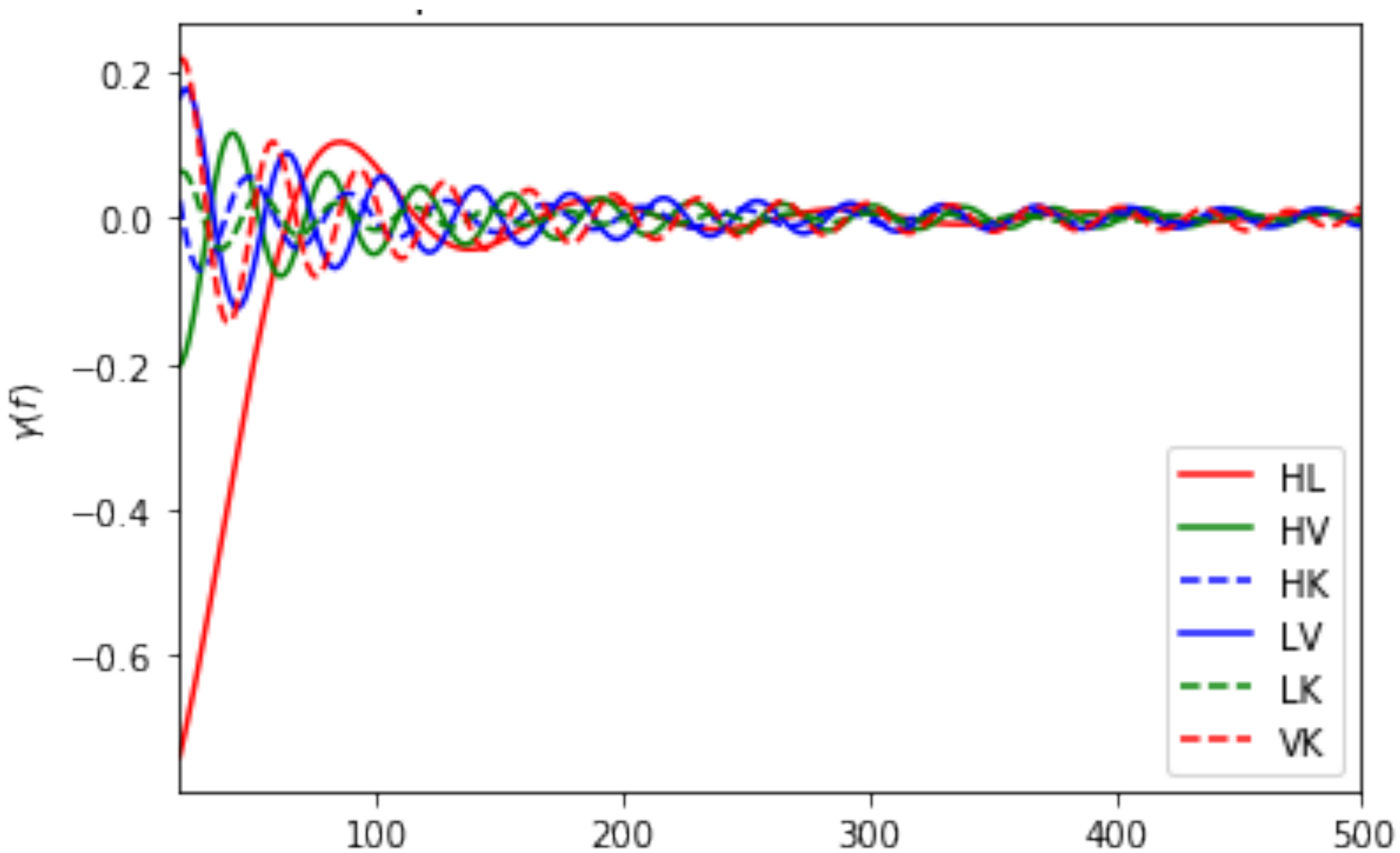

Analysis Processes

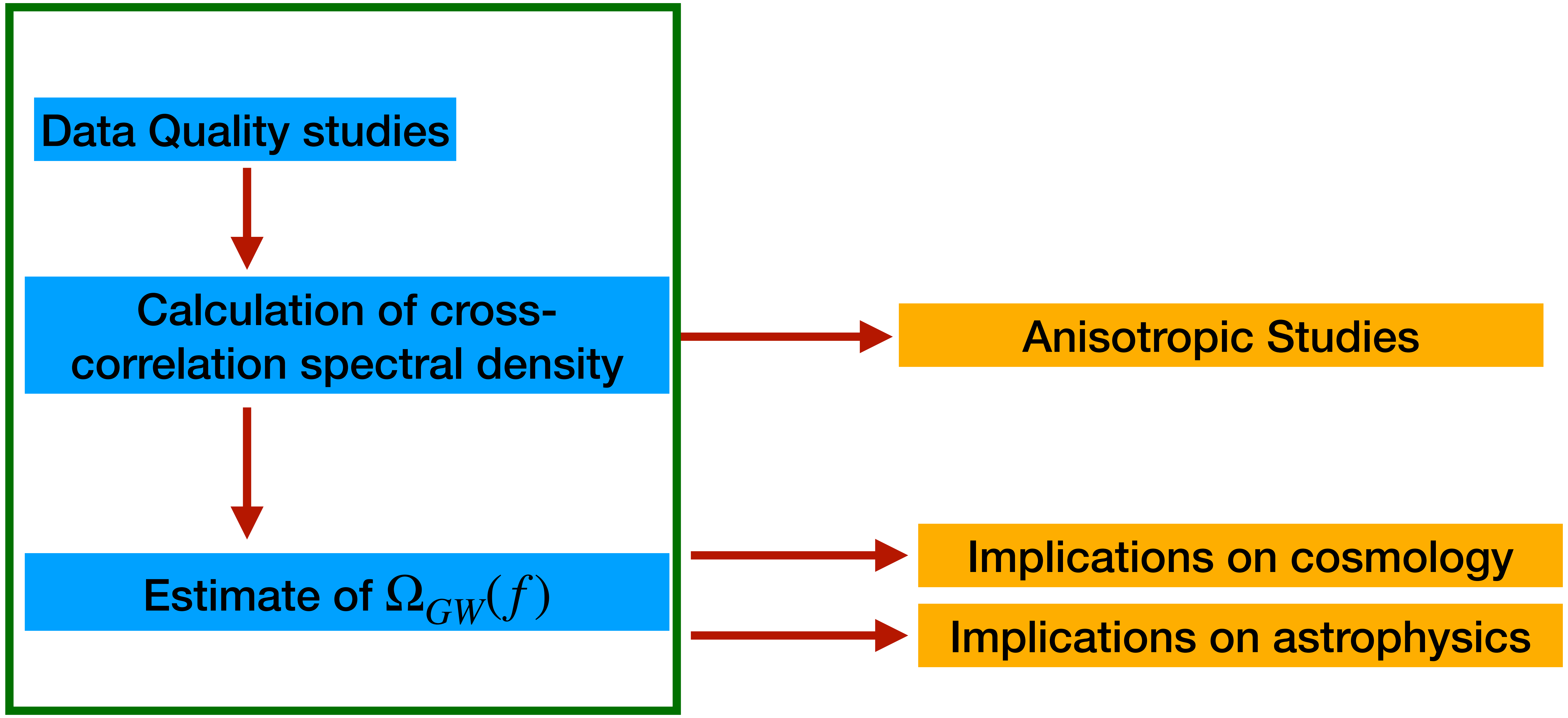

Pygwb: Isotropic Search pipeline

https://pygwb.docs.ligo.org/pygwb/

- Analyzing the data
- Run statistical checks
- Parameter estimation
- Simulate your own data

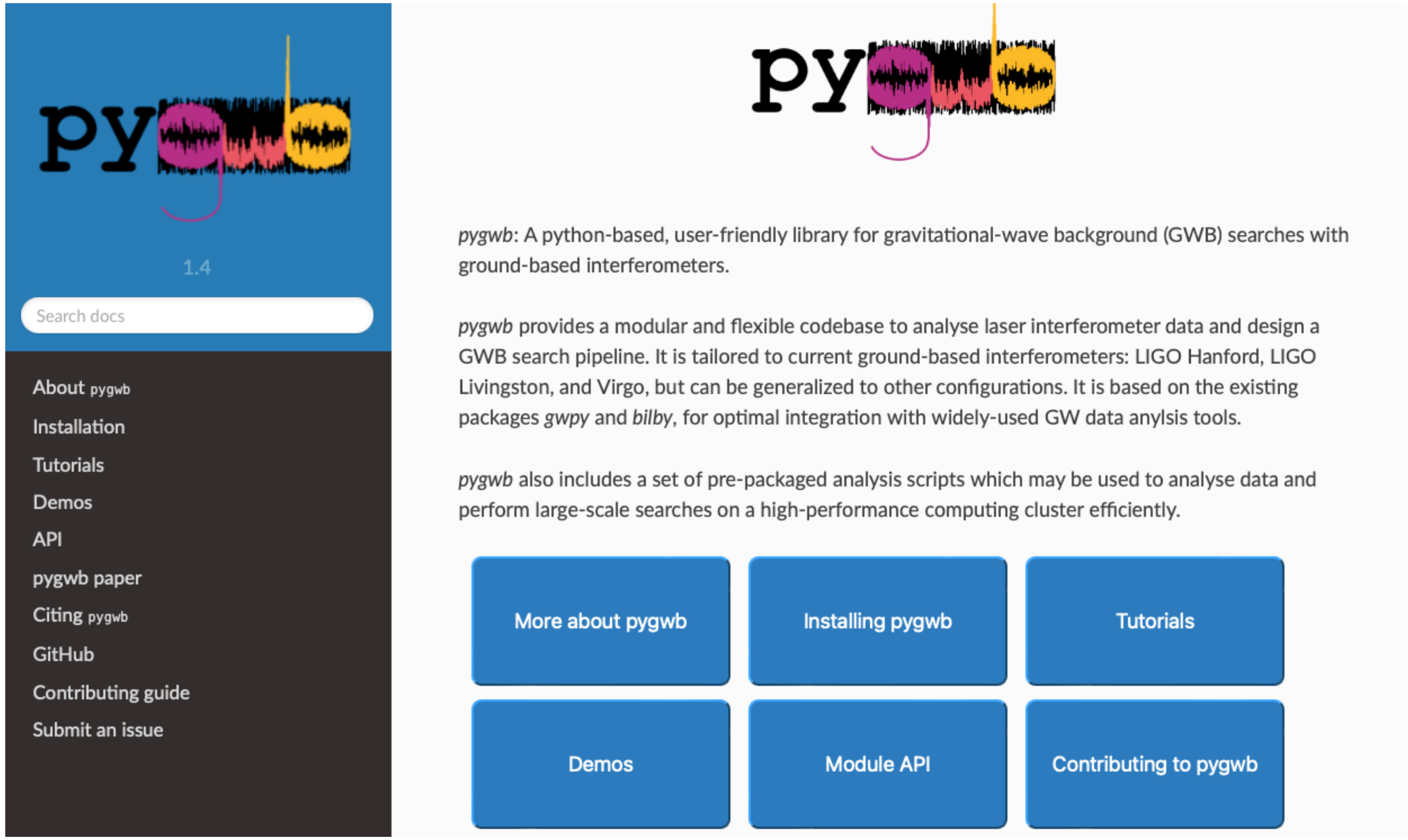

Pygwb: Isotropic Search pipeline

We define an estimator $\hat{C}_{IJ} = \frac{2}{T}\frac{\mathrm{Re}[\tilde{s}_I(f)\tilde{s}_J^*(f)]}{\Gamma_{IJ}(f)S_0(f)}$, where $S_0(f) = \frac{3H_0^2}{10\pi^2 f^3}$ and T is the duration of segment.

Uncertainty: $\sigma^2 = \frac{1}{2T\Delta f}\frac{P_I(f)P_J(f)}{\Gamma_{IJ}^2(f)S_0^2(f)}$

- Analysis parameters:
  - Duration of segments : 192 s
  - Use the Hand window for FFT and Overlap factor is 50%
  - Sampling rate: downsample from 16384 Hz to 4096 Hz
  - Coarse-grain to the frequency resolution 1/32 Hz
- Removing artifact data:
  - Applying gating scheme to remove loud glitches
  - Delta-sigma cut to remove the non-stationary
  - Notch noise lines due (calibration lines, power line harmonics, etc.)

O3 Isotropic Results

PRD 104, 022004 (2021)

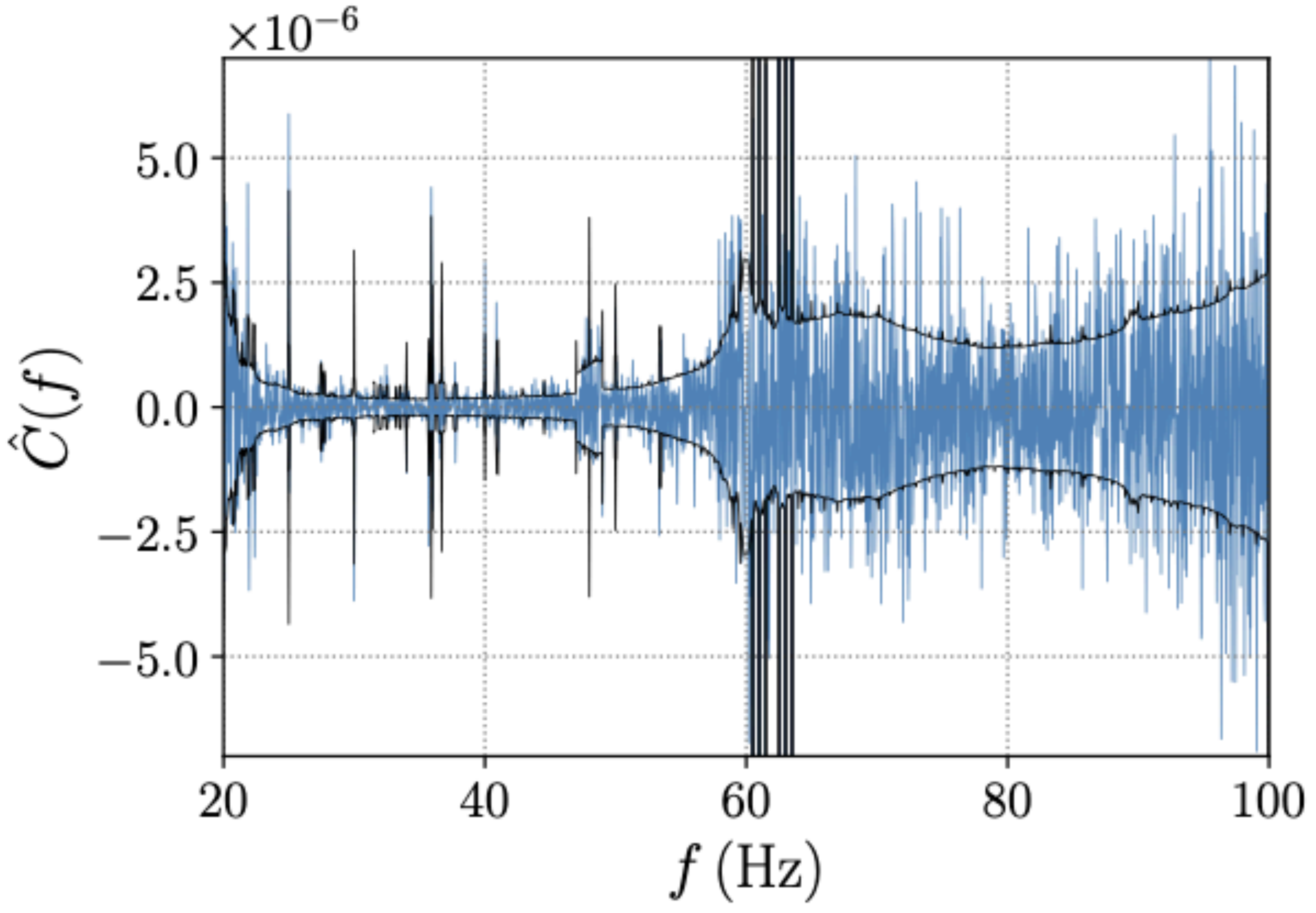

Cross-correlation spectra combining from O1-O3 (including O3 Virgo). The spectrum is consistent with expectations from uncorrelated, Gaussian noise.

O3 Isotropic Results

Upper limits on $\Omega_{gw}(f = 25Hz)$

	Uniform prior			Log-uniform prior		
α	O3	O2 [43]	Improvement	O3	O2 [43]	Improvement
0	1.7×10^{-8}	6.0×10^{-8}	3.6	5.8×10^{-9}	3.5×10^{-8}	6.0
2/3	1.2×10^{-8}	4.8×10^{-8}	4.0	3.4×10^{-9}	3.0×10^{-8}	8.8
3	1.3×10^{-9}	7.9×10^{-9}	5.9	3.9×10^{-10}	5.1×10^{-9}	13.1
Marg.	2.7×10^{-8}	1.1×10^{-7}	4.1	6.6×10^{-9}	3.4×10^{-8}	5.1

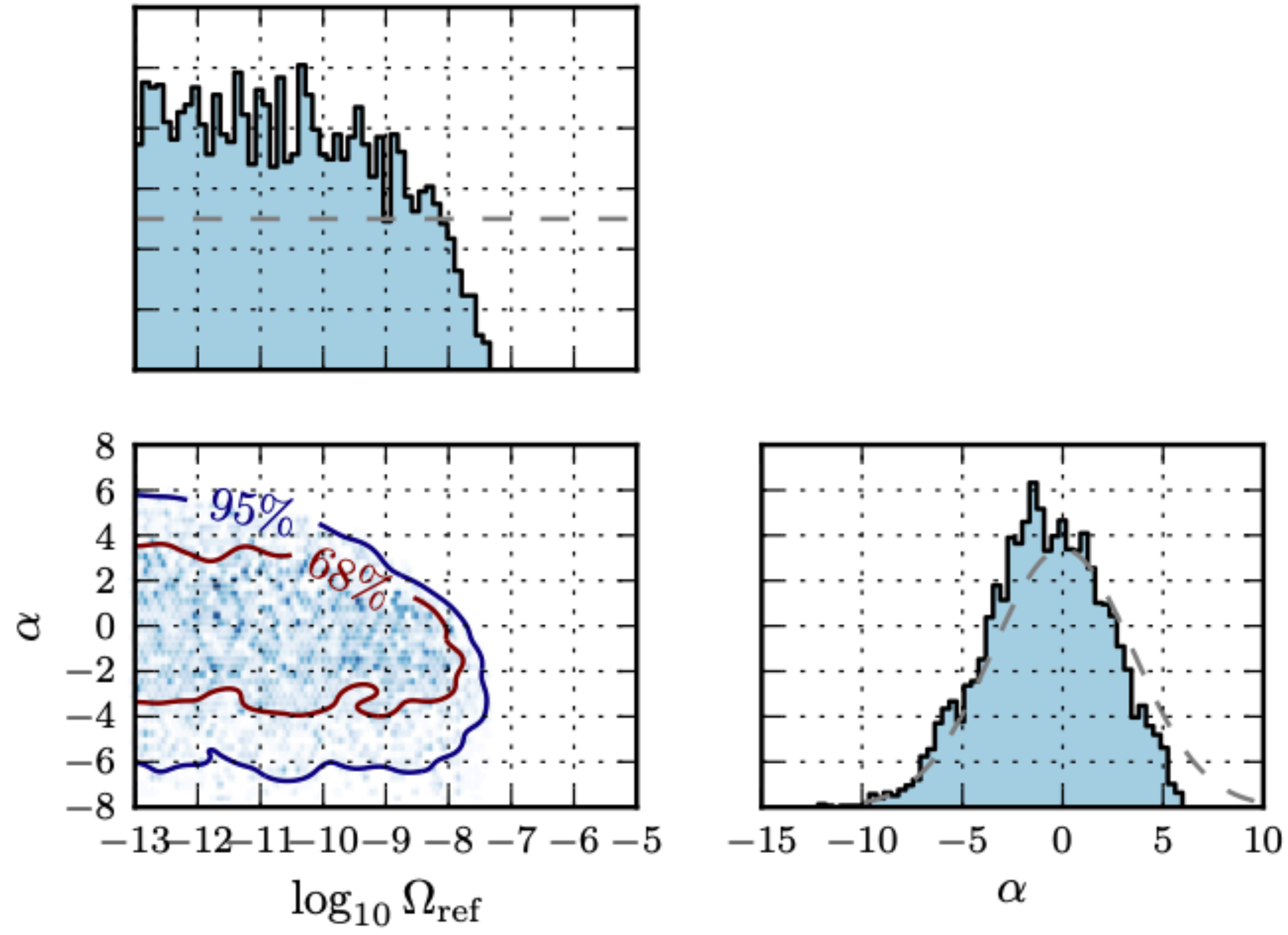

Fiducial models predictions and projected sensitivities